*Faraday Discuss.*, 1995, **101**, 51–64

# Brownian Dynamics Simulation of Particle Gel Formation: From Argon to Yoghurt

**Bert H. Bijsterbosch and Martin T. A. Bos**
*Department of Physical and Colloid Chemistry, Wageningen Agricultural University, Dreijenplein 6, 6703 HB Wageningen, The Netherlands*

**Eric Dickinson***
*Procter Department of Food Science, University of Leeds, Leeds, UK LS2 9JT*

**Joost H. J. van Opheusden**
*Department of Agricultural Engineering and Physics, Wageningen Agricultural University, Bomenweg 4, 6703 HD Wageningen, The Netherlands*

**Pieter Walstra**
*Department of Food Science, Wageningen Agricultural University, P.O. Box 8129, 6700 EV Wageningen, The Netherlands*



The influence of interparticle interactions on the fractal structure of gels formed from networks of aggregated spherical particles is investigated by Brownian dynamics computer simulation. In moderately concentrated systems of particles interacting with non-bonded Lennard-Jones interactions, restructuring of the network towards a phase-separated state leads to time-dependent changes in the primary cluster mass and in the intermediate-range fractal dimensionality. Using a colloid-type interaction potential of shorter attractive range leads to the same coarse network structure but a slower rate of restructuring. Networks derived from simulations incorporating flexible irreversible bond formation and repulsive interparticle interactions have a polymer gel character with regular spacings between chains and a small average pore size. Systems exhibiting both bonding and attractive non-bonding interparticle forces can produce permanent fine or coarse microstructures depending on the relative rates of cross-linking and phase separation. Structural features of the simulated gels have much in common with model food particle gels formed from aggregated protein particles.

A particle gel is a soft, elastic, solvent-rich material made from a network of aggregated colloidal particles. Food colloids such as yoghurt, curd and margarine are examples of particle gels; the 'particles' may consist of protein molecules (*e.g.* whey proteins), protein aggregates (*e.g.* casein micelles), protein-coated emulsion droplets, or fat crystals.[1] The formation of a dairy-type particle gel from a dispersion of milk protein 'particles' may be induced in a number of different ways (*e.g.* addition of acid, enzyme action, heating) depending on the conditions and the type(s) of protein involved. It is well known experimentally that a small change in processing conditions (like pH or temperature) can

produce a large change in the kinetics and mechanism of aggregation, and also in the microstructure and texture of the resulting gel.

The structure of a particle gel is typically rather coarse compared with the typically fine network structure of a macromolecular gel such as gelatin. In mechanical terms, the particle gel is much more brittle, and it tends to have a shorter linear elastic region and a smaller fracture strain.[2,3] While the material is necessarily uniform on the molecular scale (*i.e.* at distances smaller than the particle size) and also on the macroscopic scale (*i.e.* at the scale of specimens used in laboratory testing), the gel structure over some intermediate length scale has been recognized as being characterized by a fractal-type scaling behaviour.[4] Intuitive arguments suggest[3,5] that this fractal scaling has its origins in the fractal-type structure of precursor aggregates which join together to make up the percolating particle network. Additionally, there is the possibility that processes of gel restructuring may generate (different) fractal scaling behaviour. At its lower limit, the fractal scaling regime is expected to merge into a region of short-range liquid-like oscillatory structure like that found in simple liquids or stable concentrated dispersions.[6] The overall microstructure is likely to be ultimately dependent on the overall particle volume fraction and on the detailed nature of the particle–particle interactions during and after gelation.[7]

Computer simulation studies have shown[8–10] that the large stringy aggregates produced by irreversible cluster–cluster coagulation of colloidal particles at very low volume fraction are characterized by a single fractal dimensionality, $d_f$, when examined on length scales much larger than the individual particle size. In particular, it has been demonstrated that in three-dimensions there are two limiting fractal dimensionalities corresponding to diffusion-limited aggregation ($d_f \approx 1.8$), where clusters stick immediately on contact, and reaction-limited aggregation ($d_f \approx 2.1$), where the sticking probability is vanishingly small. The switch from diffusion-limited behaviour to reaction-limited behaviour on changing the experimental conditions (and hence the interparticle interactions) has been confirmed experimentally on model systems.[11–17] (In practice, there is usually a transition from reaction-limited to diffusion-limited fractal structure with increasing aggregate size.) Simulated (non-fractal) structure on short length scales (of the order of the individual particle diameter) is necessarily determined by excluded volume effects and short-range repulsive interactions. The presence of weak or moderate attractive interparticle forces between colliding aggregates may allow any associating clusters to 'anneal' somewhat prior to irreversible 'freezing in' of the permanent network structure.[14,18–21] Values of $d_f$ inferred from experiments[2–5] on casein particle gels are substantially higher than the idealized values quoted above for diffusion-limited or reaction-limited aggregation, possibly due to effects of aggregate restructuring and/or aggregate interpenetration at the finite particle concentration. Aggregate restructuring has been demonstrated experimentally.[2]

The simulation studies cited so far mainly refer to very low particle concentrations. At moderate volume fractions, $\phi$, more appropriate to experimental gelation, it has already been noted[6,19] that the simulated $d_f$ (inferred from the scaling of the aggregate radius of gyration) deviates significantly from the infinite dilution behaviour. While experimental studies on casein particle gels have indicated[2] consistent fractal scaling behaviour up to volume fractions as high as 0.3–0.35, it is clear that eventually, at high particle concentrations, the fractal scaling region must disappear altogether. The question arises as to what are the conditions under which particle gels can usefully by described as 'fractal'. Another related question is: how does the structure (fractal or otherwise) depend on the particle concentration and the interparticle interactions?

There have been few large-scale systematic simulation studies of the effect of $\phi$ on the structure of colloidal aggregates and particle gels. One recent exception is an off-lattice study of diffusion-limited cluster aggregation in two dimensions in which it is suggested[22] that there exist two distinct fractal scaling regimes. On a relatively short

length scale (from *ca.* four particle diameters up to some characteristic structural correlation length, $\xi$), the authors propose[22] a fractal dimensionality which is the same as the high dilution value ($d_f \approx 1.45$); on longer length scales there is another fractal dimensionality which gradually increases with $\phi$ from 1.45 up to 2.0 (the Euclidean dimensionality of the simulation space). The reason why $d_f$ does not immediately increase to 2.0 at length scales larger than $\xi$ is attributed[22] to interpenetration and/or packing of the 'fractal blobs'. For $\phi >$ *ca.* 0.25, $\xi$ becomes less than four particle diameters, and so the short-range scaling region disappears altogether. The aggregation process is then said to be 'space-limited'; that is, there is simply no space available in the system to build up proper fractal structures.

In systems with attractive interactions between the particles, another issue to be considered is (reversible) flocculation or phase separation.[23] At finite $\phi$, when the interaction strength is weak ($\varepsilon \approx kT$), the simulated system consists of reversibly formed flocs with an equilibrium fractal-type structure over medium length scales.[24] Beyond a certain percolation threshold $\phi > \phi^*$, such a system can be regarded as a very weak particle gel,[25] though the significance of the network is now really more geometrical than structural or mechanical. By analogy with a molecular fluid, as the interparticle attraction gets a little stronger ($\varepsilon \approx$ few $kT$), the flocculated dispersion becomes thermodynamically unstable with respect to phase separation into coexisting gas-like and liquid-like colloidal phases.[26] This leads to growth of dense non-fractal regions of liquid-like disorder by a process of spinodal decomposition[27] and ultimately in real systems (under gravity) to macroscopic colloid-type phase separation. When the interparticle attraction is much stronger ($\varepsilon \gg kT$), the system is still thermodynamically unstable with respect to phase separation (though the favoured condensed phase may now be a colloidal crystal[28] rather than a colloidal liquid). The rate of coarsening of the initially strongly flocculated percolating network structure may now be rather small because of the slowing down of local structural rearrangements due to the combination of strong short-range interactions and a relatively high local density. In a situation where genuinely irreversible aggregation (*i.e.* permanent particle–particle bonding) takes place between flocculating particles, the fully phase-separated state is never reached because the growing domains become geometrically 'pinned' by the cross-linking.[2,29] In practice, essentially the same situation can be envisaged in a non-bonding system for which the particle–particle attractive energy is very strong (say $> 10\ kT$). That is, owing to a geometrical pinning mechanism, a metastable glassy structure becomes 'frozen in' over timescales long compared with the simulation (or experimental) timescale.

In this paper we investigate the effect of the strength of interparticle interactions on the microstructure of particle gels generated by Brownian dynamics simulation. Emphasis is placed on the structure of percolating systems exhibiting both fractal growth and phase separation. Three different classes of model are considered. Model A (the 'argon gel' model) consists of spherical particles which interact with pairwise additive Lennard-Jones potentials of variable attractive well depth.[30] Model B (the 'bonding' model) consists of particles whose pairs can interact with weak attractive or repulsive forces, but which can also become linked together *via* flexible irreversible bonds.[7,31] Model C (the 'colloid' model) is similar to model A except that the Lennard-Jones interaction is replaced by a shorter-range potential more appropriate to colloidal particles. In each case, after starting off from a pseudo-random distribution, the simulated system of particles becomes aggregated into a dense gel-like network.

## Simulation Methodology

Consider a system of $N$ spherical particles each of mass $m$ interacting with a pairwise potential $u(r)$ where $r$ is the centre-to-centre separation. The translational Brownian

motion is described by a general Langevin-type equation of the form[32]

$$m(\mathrm{d}v_i/\mathrm{d}t) = -\sum_{j=1}^{3N} \zeta_{ij} v_j + F_i + \sum_{j=1}^{3N} \alpha_{ij} x_j; \qquad i = 1 \ldots 3N \tag{1}$$

where $t$ is time, $v_i$ is the velocity component of one particle in one direction $i$, and the sum is over all $3N$ translational degrees of freedom. The right-hand side of eqn. (1) is a sum of three forces: a hydrodynamic force which depends on a set of friction coefficients $\{\zeta_{ij}\}$, a systematic force $F_i$ which is the sum over all the interparticle forces $f(r) = -\mathrm{d}u(r)/\mathrm{d}r$ acting in direction $i$, and a stochastic force which depends on a set of Gaussian random numbers $\{x_j\}$ and another set of coefficients $\{\alpha_{ij}\}$ related to $\{\zeta_{ij}\}$ by

$$\zeta_{ij} = (kT)^{-1} \sum_k \alpha_{ik} \alpha_{jk} \tag{2}$$

When interparticle hydrodynamic interactions are neglected (as here), the configuration-dependent friction tensor $\zeta_{ij}$ is simply replaced by a constant friction coefficient

$$\zeta = 6\pi\eta a \tag{3}$$

where $\eta$ is the medium viscosity and $a$ is the particle radius. The Langevin equation then reduces to

$$m(\mathrm{d}v_i/\mathrm{d}t) = -\zeta v_i + F_i + S_i; \qquad i = 1 \ldots 3N \tag{4}$$

where $S_i$ is the fluctuating force describing random-walk motion in direction $i$ for a particle with an Einstein-type diffusion coefficient

$$D = kT/\zeta \tag{5}$$

A Brownian dynamics 'moving-on' algorithm based on eqn. (4) has the form

$$\Delta r_i(\Delta t) = \zeta^{-1} F_i \Delta t + R_i(D, \Delta t); \qquad i = 1 \ldots 3N \tag{6}$$

where $\Delta r_i(\Delta t)$ is the overall change in particle position in direction $i$ during the timestep $\Delta t$, and $R_j(D, \Delta t)$ is the random translational displacement of a particle with diffusion coefficient $D$ during the time interval $\Delta t$. An important requirement for eqn. (6) to be valid is that $\Delta t$ should be large compared with the characteristic timescale of solvent molecular motion, but also small enough to ensure that the force $F_i$ remains effectively constant when the particle position changes from $r_i(t)$ to $r_i(t + \Delta t)$.

In simulations of type B where some individual particles become bonded (or otherwise irreversibly aggregated together), it is also necessary to monitor their rotational motion in order to describe the multi-particle dynamical behaviour properly. A Langevin-type equation analogous to eqn. (1) can be written down[33] for the rotational Brownian motion. In the absence of interparticle hydrodynamic interactions, the rotational and translational motions are decoupled.[34] So the 'moving-on' routine for torque-free independent particle rotation has the simple form

$$\Delta\theta_i(\Delta t) = R_i^{\mathrm{R}}(D^{\mathrm{R}}, \Delta t); \qquad i = 1 \ldots 3N \tag{7}$$

where $\Delta\theta_i = R_i^{\mathrm{R}}$ is the random rotational displacement in direction $i$ for a particle with rotational diffusion coefficient $D^{\mathrm{R}} = 3D/4a^2$, and the sum now is over all $3N$ rotational degrees of freedom.

In model A we assume[30] that particle pairs interact with a Lennard-Jones potential of the form

$$u(r) = 4\varepsilon[(\sigma/r)^{12} - (\sigma/r)^6] \tag{8}$$

where $\sigma$ is the collision diameter [*i.e.* the value of $r$ where $u(r) = 0$] and $\varepsilon$ is the maximum attractive energy [*i.e.* $u(r) = -\varepsilon$ and $f(r) = 0$ at $r_{\min} = 2^{1/6}\sigma$]. The potential is

set to zero for $r > 2.5\ \sigma$ to improve computational efficiency. The hydrodynamic radius of the particle is arbitrarily set at $a = \frac{1}{2}\ \sigma$.

In model B we assume[7] that particles can form irreversible flexible linkages with other particles that approach to within a certain bonding distance (*i.e.* $r < d_{\text{bond}}$). The rate of reaction is expressed in terms of a probability, $P_{\text{bond}}$, that a bond will form during time interval $\Delta t$. Once a bond is formed, it cannot be broken and the angle(s) between two (or more) bonds on the same particle cannot change. The subsequent relative particle motion is restricted such that the surface-to-surface bond length does not exceed the maximum specified bond length $h_{\text{bond}} = d_{\text{bond}} - 2a$. The generation of new configurations is subject to both the excluded volume and the maximum bond length constraints. In addition to being able to form permanent bonds, the model B particle pairs interact with a distance-dependent force of the form

$$f(r) = \begin{cases} \infty; & r < 2a \\ -w; & 2a \leqslant r < d_{\text{max}} \\ 0; & r > d_{\text{max}} \end{cases} \tag{9}$$

where $w$ is an interaction strength parameter, which can be attractive ($w > 0$) or repulsive ($w < 0$), and $d_{\text{max}}$ is the maximum range of the particle–particle interaction.

In model C we assume that, when the distance-dependent force is attractive [*i.e.* $f(r) < 0$], the particle pairs interact with a shifted version of the potential form

$$u(r) = (c_1 r)^{-12} - c_2 r^{-2} + c_3 \exp(-c_1 r); \qquad r > r_{\text{min}} \tag{10}$$

with coefficients $c_1$, $c_2$ and $c_3$ set to give $u(r) = -\varepsilon$ at $r = r_{\text{min}}$. When the force is repulsive [$f(r) > 0$], the model C particles are assumed to interact with the repulsive part of the Lennard-Jones potential [eqn. (8)]. The energy and force are both continuous functions of $r$, but, unlike the full Lennard-Jones potential, the model C interaction has a shorter finite attractive range [*i.e.* $u(r) = 0$ and $f(r) = 0$ for $r/\sigma > 1.2205$]. (In practice, the attractive range may be as short as $r/\sigma \approx 1.01$ for μm-sized particles, and so the range of the assumed model C potential may actually be realistic only for rather small colloidal particles.)

## Fractal Analysis

In a particle gel formed by irreversible aggregation of spherical particles, three spatial scales of structure may be expected:[6] (i) short-range order from packing and excluded volume effects, (ii) medium-range disorder associated with the ramified structure of the aggregating clusters, and (iii) long-range uniformity for a homogeneous material. In terms of the particle–particle distribution function $g(r)$, the three regions are associated with (i) strong damped liquid-like oscillations out to a few particle diameters ($r < r_0$), (ii) a fractal scaling regime with

$$g(r) \sim (r/\xi)^{d_f - 3}; \qquad r_0 \leqslant r \leqslant \xi \tag{11}$$

and (iii) a non-fractal uniform structure with $g(r) \equiv 1$ beyond some characteristic correlation length $\xi$.

In estimating an effective $d_f$ from the simulations, it is convenient to smooth out the short-range oscillations in $g(r)$ by calculating the integrated pair distribution function

$$n(r) = 4\pi\rho_0 \int_0^r s^2 g(s)\ \mathrm{d}s \tag{12}$$

where $\rho_0$ is the average particle number density and $n(r)$ is the average number of particles within range $r$ of another particle. $d_f$ can be determined from the slope of the linear region of a plot of log $n(r)$ *vs.* log $r$. For large length scales ($r > \xi$) we have $n(r) \sim r^3$ and

$d_f \equiv 3$. The $d_f$ of the intermediate regime is only one aspect of the gel structure. Also important is the scaling prefactor $n_0$ in

$$n(r) = n_0(r/r_0)^{d_f} \tag{13}$$

where $r_0$ is some arbitrary length scale. If we take $r_0$ as the primary particle radius (*i.e.* $\sigma/2$ in models A and C, or $a$ in model B), $n_0$ becomes the rescaled mass of the primary particle. The value of $n_0$ is a measure of the average number of particles in the primary clusters from which the fractal scaling regime is built, and a large value of $n_0$ indicates a coarse microstructure. On the other hand, for large values of $r$, one must have

$$n(r) = \phi(r/r_0)^3 \tag{14}$$

We find $n_0 = \phi$ if we artificially extend the homogeneous scaling regime to the primary particle scale. Low values of $n_0$ (possibly even less than unity) imply open structures. The crossover between the fractal scaling regime and the homogeneous regime takes place at the correlation length $\xi$:

$$n_0(\xi/r_0)^{d_f} = \phi(\xi/r_0)^3 \tag{15}$$

$$\xi = r_0(\phi/n_0)^{(d_f-3)^{-1}} \tag{16}$$

For 'classical' cluster–cluster aggregation (no local reorganization or phase separation) with $r_0 = a = \sigma/2$ and $n_0 = 1$, eqn. (16) reduces to[3]

$$\xi \approx a\phi^{(d_f-3)^{-1}} \tag{17}$$

## Simulation Results and Discussion

Brownian dynamics simulations have been carried out[30] in three dimensions with periodic boundary conditions on systems of model A particles with parameter values corresponding to $N = 1000$, $\sigma = 1$ μm, $\eta = 1$ mPa s, $T = 298$ K and $\Delta t = 3.44$ ms. Percolating networks were generated at volume fractions above $\phi \approx 0.07$. The aggregated structures were analysed after various times up to $t = 1.1 \times 10^3$ s (*i.e.* $3.2 \times 10^5$ timesteps) in simulation runs on systems with well depths of $\varepsilon = 2\ kT$ or $4\ kT$ and volume fractions of $\phi = 0.09$, 0.11 or 0.13. The following quantities were calculated: $g(r)$, $n(r)$, $d_f$ and $n_0$.

Fig. 1 shows derived values of $n_0$ and $d_f$ as a function of $\phi$ and the number of timesteps, $n_{step}$. Note that there is no universal fractal scaling behaviour in these systems. The systems are thermodynamically unstable with respect to gas–liquid phase separation. With increasing simulation time, there is a tendency for $n_0$ to increase, indicating a process of short-range densification; there is also a tendency for $d_f$ to decrease, indicating a process of medium-range stringly cluster formation. A qualitatively similar effect of aggregate ageing on gel structure has recently been reported by van Garderen *et al.*[22] An increase in the maximum attractive energy of the Lennard-Jones potential from $\varepsilon = 2\ kT$ to $\varepsilon = 4\ kT$ leads to a substantial increase in $n_0$ and a substantial reduction in $d_f$. The time evolution of the primary close-packed cluster radius seems to be relatively insensitive to $\phi$. The same is certainly not true, however, for the time evolution of $d_f$, especially for the system with $\varepsilon = 4\ kT$.

Under conditions of thermodynamic phase separation, the percolating clusters have a transient character. The process of short-range densification induces the formation of a coarser blob-like structure with larger voids and the elongation and/or breaking of some existing aggregate branches. This is in accordance with a simultaneous increase in $n_0$ and decrease in $d_f$. We explain the decrease in $d_f$ by noting that it is more likely that particles necessary for the increase in $n_0$ are moved from intermediate length scales (the fractal scaling regime) than from long length scales (the homogeneous region). Therefore

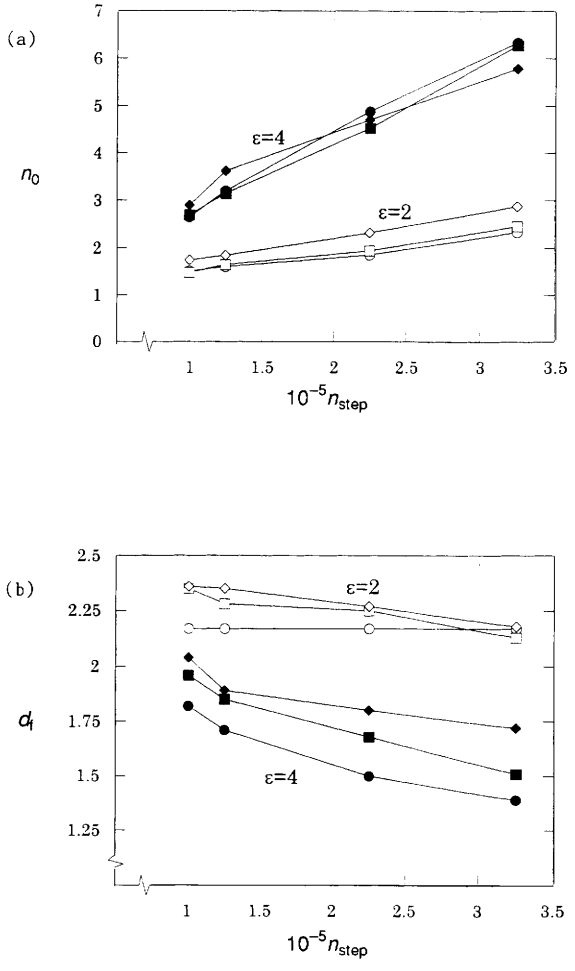


**Fig. 1** Time-dependent structure of simulated model A particle gels. The plots show fitted values of (a) $n_0$ and (b) $d_f$ as a function of $\varepsilon$ and $\phi$. The quantities $n_0$ and $d_f$ are plotted against $n_{step}$; ◇, $\phi = 0.09$; □, $\phi = 0.11$; ○, $\phi = 0.13$. Open symbols: $\varepsilon = 2\ kT$; filled symbols, $\varepsilon = 4\ kT$.

the structure on intermediate length scales must become more stringy (*i.e.* a lower value of $d_f$). Increasing the well depth increases the rate of formation of the initial percolated network and also the rate of reorganization (though not necessarily to the same extent). As expected, for larger values of $\varepsilon$, the reorganized clusters become more closely packed on short length scales. It is likely that the time-dependent evolving structure will depend on the shape of the interparticle potential as well as on the well depth. The (molecular) Lennard-Jones potential strongly favours local structural reorganization because it has a rather broad interaction range. A more realistic colloidal potential, for instance one based on the well known DLVO potential form,[1] has a steeper repulsion and a much shorter attractive range (relative to the particle size), *i.e.* more like model C [eqn. (10)].

We turn next, however, to the situation in which the extent of thermodynamically driven structural reorganization is permanently restricted by irreversible bond formation. Brownian dynamics simulations have been carried out[7] in two dimensions on periodic systems of model B particles with $N = 400$, $\phi = 0.35$, $a = 1$, $d_{max} = 4$, $h_{bond} = 0.3$, $D = 1.0$ and $\Delta t = 0.005$. Structures were typically analysed at $t = 150$ (*i.e.* after

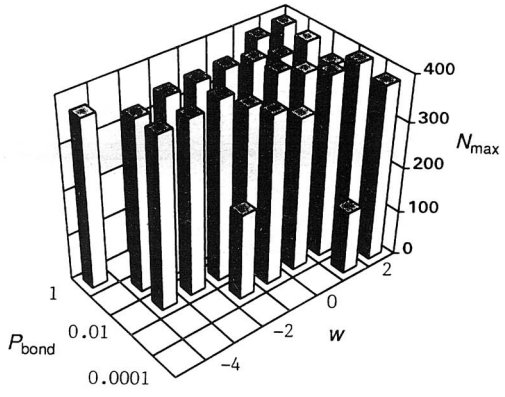


(a)

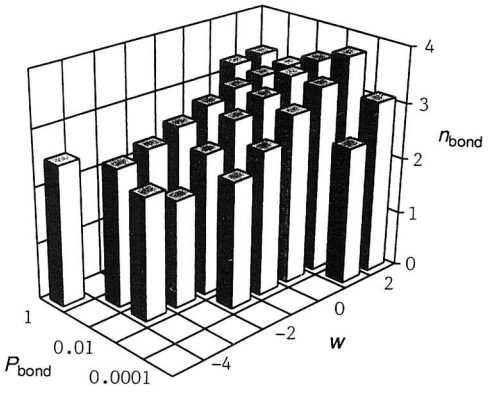


(b)

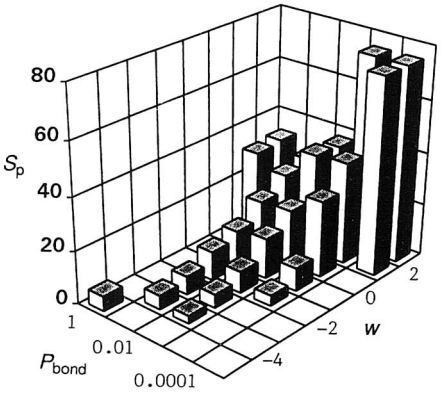


(c)

**Fig. 2** Characteristics of two-dimensional model B particle gels generated as a function of $w$ and $P_{bond}$: (a) $N_{max}$ (b) $n_{bond}$ (c) $S_p$ (arbitrary units)

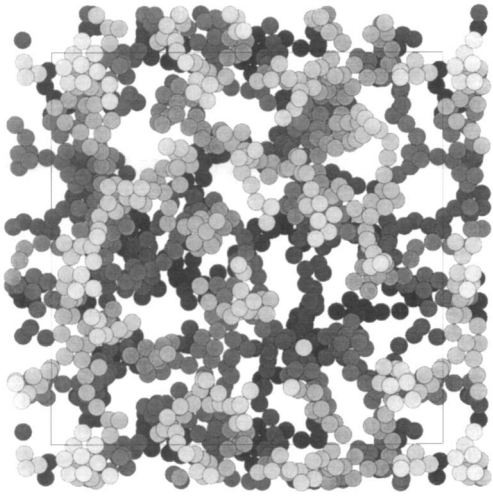

**Fig. 3** Snaphot picture of three-dimensional network structure produced from simulated aggregation of model **B** particles (after $2.1 \times 10^5$ timesteps) with $\phi = 0.05$, $w = 0$ and $P_{bond} = 1.0$. The darkest particles lie furthest away from the observer.

$3 \times 10^4$ timesteps) for various simulations runs with values of the interaction strength parameter set in the range $-5 \leqslant w \leqslant 2$ and values of the bonding probability set in the range $10^{-4} \leqslant P_{bond} \leqslant 1.0$. The following quantities were calculated: $N_{max}$, the number of particles in the largest aggregate; $n_{bond}$, the average number of bonds per particle and $S_p$, the average pore size.

To simulate a permanent cross-linked gel, it is necessary for all or most of the particles to become part of a single large aggregate that spans the basic simulation cell. We see in Fig. 2(a) that this condition is satisfied (*i.e.* $N_{max} \rightarrow N$) for most the values of $w$ and $P_{bond}$ investigated. (Simulation times longer than $t = 150$ are required to generate a percolated network if the bonding probability is very low or if the interparticle interaction is very strongly repulsive.) The quantity $n_{bond}$ is a measure of the mean local coordination number of the particles in the network. The data in Fig. 2(b) show that there is a systematic increase in $n_{bond}$ with increasing $w$. This is because gel systems with substantial repulsive interactions ($w \leqslant -3$) contain wiggly linear chains of low average particle coordination number ($n_{bond} \rightarrow 2$), whereas gel systems with attractive interactions ($w \geqslant 1$) contain close-packed regions of relatively high average coordination number ($n_{bond} > 3$). Fig. 2(c) shows that there is a large increase in $S_p$ as the interaction parameter changes from repulsive to attractive. Reduction in $P_{bond}$ favours a fine-pore structure when the particle–particle interaction force is repulsive, but the opposite is the case when the force is attractive.

Substantial net repulsive particle interactions lead to strong chain–chain repulsion during cross-linking. This inhibits multi-particle bonding, maximizes particle–solvent interactions, and generates a maze-like pore structure with average spacing of the order of the range of the interparticle repulsion. Because single bonds are quite flexible in this model, the gel structure generated with $w \ll 0$ has some of the mechanical and swelling characteristics of a typical polymer gel. That is, owing to the flexibility of the highly solvated chains, so long as the individual particle segments on the chains are reasonably small (say 10 nm), one expects a substantial entropic contribution to the macroscopic elastic properties of the gel. In contrast, attractive particle interactions cause flocculation into close-packed clusters prior to irreversible cross-linking. This encourages multi-particle bonding ($n_{bond}$ increases), maximizes particle–particle interactions at the expense

of particle–solvent interactions, and generates a pore structure with average spacing very much greater than the monomer particle size. Such a coarse rigid gel would be expected to have macroscopic elastic behaviour dominated by energetic factors.[7] On the other hand, if the particles are very reactive ($P_{bond} \sim 1$), they do not have sufficient time to rearrange into close-packed clusters prior to bonding; the structure of the gel is now entirely kinetically controlled. It is interesting to note that, in this case, even though the rate of bonding ($\propto P_{bond}$) is higher, there is a lower overall density of cross-links ($\propto n_{bond}$) in the final network. This also has implications for gel elasticity.

Computations have also been carried out in three dimensions on systems of model B particles with $N = 1000$, $d_{max} = 3a$, $h_{bond} = 0.1a$, $D = 1.0$, $\Delta t = 0.001$ and $\phi = 0.05$, 0.07 and 0.1. Structures were typically analysed at various times up to $t = 50$ (*i.e.* $5 \times 10^4$ timesteps) for simulation runs with $P_{bond} = 1.0$ and $w = -1$, 0 or $+1$. Based on visual inspection of the pictures of the gel structures, the trends of behaviour seem to be in good qualitative agreement with the previous two-dimensional results. Fig. 3 shows a pictorial representation of the gel structure obtained with $w = 0$ and $\phi = 0.05$ after $t = 10$. The plot of log $n(r)$ *vs.* log $r$ in Fig. 4 for the same system shows a rather limited fractal scaling regime ($d_f \approx 1.9$ up to $\xi \approx 7a$). In contrast to model A, we see that, even at low volume fraction, model B with rapid cross-linking ($P_{bond} = 1.0$) and no interactions ($w = 0$) produces a thin-stranded network structure ($n_0 = 0.5$) having a fine-pore distribution but no dominant fractal character in the scaling of $n(r)$.

The kinetic balance between phase separation and cross-linking may also influence the microstructure of mixed particle gels.[31] To investigate such behaviour, we have extended the model B simulations to a binary two-dimensional mixture of equal sized particles (1 and 2). The system is characterized by three separate pair parameters $w_{11}$, $w_{22}$ and $w_{12}$ corresponding to the 1–1, 2–2 and 1–2 interactions and a contant $P_{bond}$ for all the reacting pairs. Fig. 5 shows some results for an equimolar mixture with $N = 720$, $\phi = 0.35$, $d_{max} = 4a$, $h_{bond} = 0.3a$, $D = 1.0$, $\Delta t = 0.005$, $t = 250$, $w_{11} = 0$, $w_{22} = 0$ and $w_{12} = -4$. The relative density of 1–2 particle pairs, $n_{12}(r)$, is plotted against $r$ for three different values of $P_{bond}$. When the rate of cross-linking is high ($P_{bond} = 10^{-1}$), the function $n_{12}(r)$ has sharp peaks at $r \approx 2a$, $4a$ and $6a$, corresponding to a mixed gel network with little compositional heterogeneity on length scales larger than the particle diameter. When the cross-linking rate is an order of magnitude lower ($P_{bond} = 10^{-2}$) the beginnings of local phase separation start to become evident in the $n_{12}(r)$ data: the height of the peak at $r \approx 2a$ is greatly reduced, indicating a considerable loss of 1–2 nearest

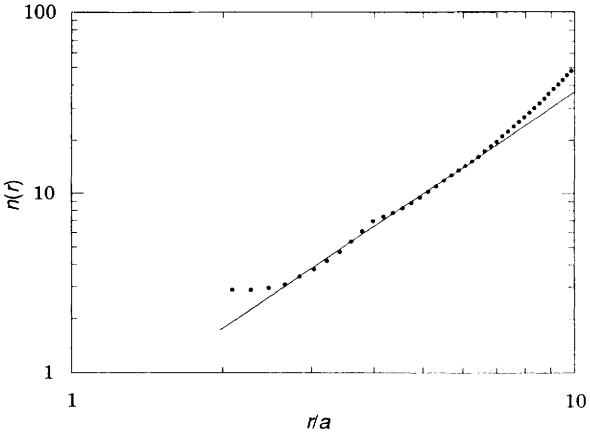


**Fig. 4** Scaling analysis of $n(r)$ for system illustrated in Fig. 3. The points are the simulation data. The slope of the fitted straight line on the log–log plot gives the intermediate range $d_f = 1.9$.

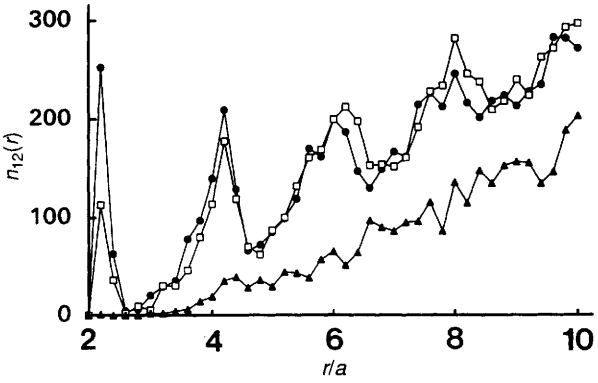


**Fig. 5** Influence of rate of cross-linking on the two-dimensional structure of mixed model B particle gels with $w_{11} = w_{22} = 0$ and $w_{12} = -4$. The number of unlike particle pairs (in interval $0.2a$), $n_{12}(r)$, is plotted against $r$: ●, $P_{\text{bond}} = 10^{-1}$; □, $P_{\text{bond}} = 10^{-2}$; ▲, $P_{\text{bond}} = 10^{-5}$.

neighbour pairs at the expense of 1–1 or 2–2 pairs. When the cross-linking rate is very low ($P_{\text{bond}} = 10^{-5}$), the function $n_{12}(r)$ is effectively zero for $r < 4a$, and it increases monotonically with $r$ thereafter (within the statistical error). This plot is consistent with rather extensive phase separation in an aggregation system exhibiting liquid–liquid incompatibility (segregation) on a timescale short compared with the timescale for particle cross-linking. Taken together with detailed simulation snapshots,[31] the data in Fig. 5 are a reflection of the fact that, once the size of bonded clusters becomes similar to that of micro-phase-separating domains, the process of compositional reorganization is halted. A similar type of behaviour is expected in three dimensions, albeit with a much greater degree of self-connectivity (bicontinuous structure) amongst the 'frozen-in' domains of similar composition.

Finally, we report preliminary results in three dimensions for systems of model C particles with values of well depth $\varepsilon$ in the range 2–10 $kT$ and volume fractions in the range $0.07 \leqslant \phi \leqslant 0.15$. The model C interaction potential is of much shorter attractive

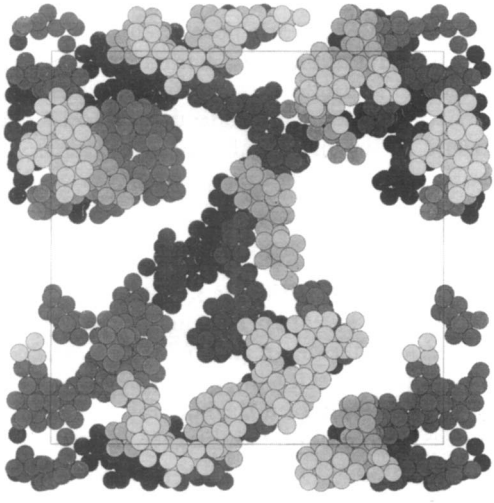

**Fig. 6** Snapshot picture of three-dimensional network structure produced from simulated aggregation of model C particles (after $1.9 \times 10^6$ timesteps) with $\phi = 0.11$ and $\varepsilon = 4\,kT$

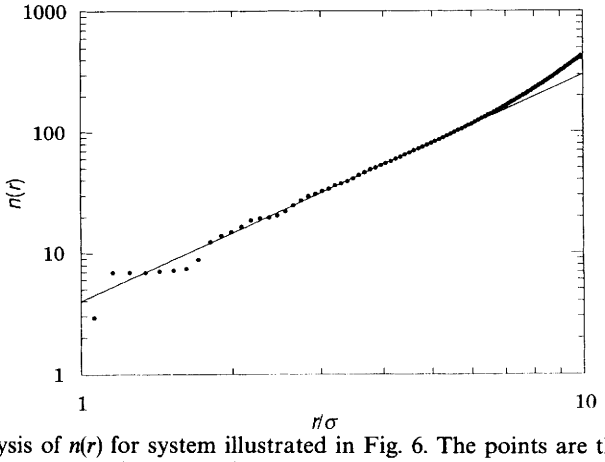


**Fig. 7** Scaling analysis of $n(r)$ for system illustrated in Fig. 6. The points are the simulation data. The slope of the fitted straight line on the log–log plot gives the intermediate range $d_f = 1.9$.

range (with respect to the particle size) than the model A Lennard-Jones potential. Fig. 6 is a pictorial representation of the gel structure obtained after a simulation time of $n_{step} = 10^5$ in a system with $\phi = 0.112$ and $\varepsilon = 4\ kT$. Fig. 7 is a plot of log $n(r)$ *vs.* log $r$ for the same system; the straight line fit gives an effective $d_f = 1.9$ and $n_0 = 2.0$. These latter values are in fact rather close to those obtained with model A under similar conditions (see Fig. 1).

Note that the structures illustrated in Fig. 4 and 6, while looking quite different by eye, both have the same intermediate range $d_f$. In contrast to the fine particle-bonded structure ($n_0 = 0.5$) illustrated in Fig. 4, the picture in Fig. 6 is typical of a coarse phase-separated gel ($n_0 = 2$) in the early stages of cluster densification. The very different appearance of the two network structures in terms of porosity and strand thickness indicates the danger of blindly adopting the fractal dimensionality as a single parameter to describe the structure of simulated particle gels. (Presumably this comment is equally applicable to some real particle gels.) As we are in the two-phase region, and there are no bonds forming to 'cement' the network permanently, the model C gel structure is undoubtedly time-dependent but, unlike the Lennard-Jones 'argon gel', the rate of restructuring of this 'colloid gel' is quite slow compared with the total simulation time. The structure also appears to be more senstive to $\phi$ than to the well depth. Increasing $\phi$ to 0.132 leads to an increase in the fitted value of $d_f$ to *ca.* 2.1 (for either $\varepsilon = 2\ kT$ or $\varepsilon = 10\ kT$).

## Conclusions

The particle gel simulations reported in this paper have explored the effects of particle interactions and volume fraction on network structure. Whereas structures formed by 'classical' irreversible cluster–cluster aggregation at low particle concentrations are characterized by a constant time-invariant fractal dimensionality on intermediate length scales ($d_f$ in the range 1.8–2.1 depending on the sticking probability), this in not the case with more complicated forms of interactions at higher concentrations. For such systems the value of $d_f$, obtained for instance by fitting the integrated pair distribution function $n(r)$ over an intermediate range of $r$ values, does not give by itself a full description of the microstructure of the particle gel. It is clear that other structural parameters must also be considered, such as the short-scale primary cluster mass or the average pore size.

When the volume fraction in the simulated system reaches $\phi \approx 0.3$ or above, we cease to find a convincing fractal scaling regime at all.

With moderate or strong (non-bonding) attractive interactions between the particles, any inferred fractal character is necessarily time-dependent because the system is ultimately thermodynamically unstable with respect to gas–liquid phase separation (or liquid–liquid phase separation in a segregating binary system). The rate of restructuring, as measured by the rate of increase of $n_0$, depends on the range of the attractive interactions. It is faster for a hypothetical argon gel composed of 'slippy' Lennard-Jones molecules than for a model yoghurt-like colloid gel composed of 'sticky' protein particles (casein micelles). Real systems like those containing milk protein particles often have strong molecular interactions generated during restructuring. Nevertheless, despite this complexity, for reasons that are not fully clear, the macroscopic properties of such systems (permeability, elastic modulus, *etc.*) have been shown[2–5] to be well described by single parameter fractal scaling over a wide range of volume fractions. Unfortunately, we have to conclude that, so far, we have not been able to establish a convincing quantitative link between the 'experimental' fractal dimensionalities determined previously for casein particle gels[2–5] and the restructuring processes generated in our simple particle gel simulations.

The bonding model represents the extreme case in which permanent cross-links are formed leading eventually to a strong covalently bonded network. A fine-pore cross-linked structure is produced when the interparticle pair interaction is neutral or (especially) net repulsive. The resulting microstructure may actually possess little or no fractal character, particularly when $\phi$ is high and the spacing between particle chains is rather narrow and regular. In such a system, once considerable cross-linking has occurred between repulsively interacting particles, there is little aggregate diffusion, and restructuring becomes limited to slow permanent 'handshakes' between flexible extending arms. Such cross-links may not have much effect on the structural scaling behaviour, but they could be extremely important in relation to the rheology of the ageing gel. This contrasts with the possibility of extensive time-dependent structural changes in the non-bonding situation, where some initially formed aggregates may thin out or break up, whilst others coarsen under the persistent drive towards phase separation. On the other hand, the combination of bond formation and attractive (non-bonded) interactions ultimately produces a constant microstructure of variable coarseness (depending on the relative rates of particle bonding and cluster compactification). This is due to the growth of coarsening domains eventually being halted in its tracks by the increasing accumulation of structure-reinforcing cross-links.

We acknowledge valuable discussions with T. van Vliet during the course of this project. E.D. is grateful to Wageningen Agricultural University for the award of a Visiting Senior Fellowship during the period in which some of this research was carried out.

## References

1 E. Dickinson, *An Introduction to Food Colloids*, Oxford Univerity Press, Oxford, 1992.
2 L. G. B. Bremer, Ph.D. Thesis, Wageningen Agricultural University, 1992.
3 P. Walstra, T. van Vliet and L. G. B. Bremer, in *Food Polymers, Gels and Colloids*, ed. E. Dickinson, Royal Society of Chemistry, Cambridge, 1991, p. 369.
4 L. G. B. Bremer, B. H. Bijsterbosch, R. Schrijvers, T. van Vliet and P. Walstra, *Colloids Surf.*, 1990, **51**, 159.
5 L. G. Bremer, B. H. Bijsterbosch, P. Walstra and T. van Vliet, *Adv. Colloid Interface Sci.*, 1993, **46**, 117.
6 E. Dickinson, *J. Colloid Interface Sci.*, 1987, **118**, 286.
7 E. Dickinson, *J. Chem. Soc., Faraday Trans.*, 1994, **90**, 173.
8 H. J. Herrmann, *Phys. Rep.*, 1986, **136**, 153.
9 R. Jullien, *Contemp. Phys.*, 1987, **28**, 477.

10 P. Meakin, in *Phase Transitions and Critical Phenomena*, ed. C. Domb and J. L. Lebowitz, Academic Press, London, 1988, vol. 12, p. 335.
11 D. A. Weitz, J. S. Huang, M. Y. Lin and J. Sung, *Phys. Rev. Lett.*, 1984, **53**, 1657; 1985, **54**, 1416.
12 C. Aubert and D. S. Cannell, *Phys. Rev. Lett.*, 1986, **56**, 738.
13 G. Bolle, C. Cametti, P. Codasterfano and P. Tartaglia, *Phys. Rev. A*, 1987, **35**, 837.
14 M. Y. Lin, R. Klein, H. M. Lindsay, D. A. Weitz, R. C. Ball and P. Meakin, *J. Colloid Interface Sci.*, 1990, **137**, 263.
15 P. W. J. G. Wijnen, T. P. M. Beelen, C. P. J. Rummens and R. A. van Santen, *J. Non-Cryst. Solids*, 1991, **136**, 119.
16 M. Carpinetti and M. Giglio, *Adv. Colloid Interface Sci.*, 1993, **46**, 73.
17 P. W. Zhu and D. H. Napper, *Phys. Rev. E*, 1994, **50**, 1360.
18 G. C. Ansell and E. Dickinson, *Phys. Rev. A*, 1987, **35**, 2349.
19 G. C. Ansell and E. Dickinson, *Faraday Discuss. Chem. Soc.*, 1987, **83**, 167.
20 E. Dickinson and C. Elvingson, *J. Chem. Soc., Faraday Trans. 2*, 1988, **84**, 775.
21 P. Meakin, *J. Colloid Interface Sci.*, 1990, **134**, 235.
22 H. F. van Garderen, W. H. Dokter, T. P. M. Beelen, R. A. van Santen, E. Pantos, M. A. J. Michels and P. A. J. Hilbers, *J. Chem. Phys.*, 1995, **102**, 480.
23 E. Dickinson, *Annu. Rep. C*, Royal Society of Chemistry, London, 1983, p. 3.
24 E. Dickinson, C. Elvingson and S. R. Euston, *J. Chem. Soc., Faraday Trans. 2*, 1989, **85**, 891.
25 E. Dickinson, *Chem. Ind.*, 1990, 595.
26 J. A. Long, D. W. Osmond and B. Vincent, *J. Colloid Interface Sci.*, 1973, **42**, 545.
27 J. W. Cahn, *J. Chem. Phys.*, 1965, **42**, 93.
28 P. Pieranski, *Contemp. Phys.*, 1983, **24**, 25.
29 F. Sciortino, R. Bansil, H. E. Stanley and P. Alstrøm, *Phys. Rev. E*, 1993, **47**, 4615.
30 M. T. A. Bos and J. H. J. van Opheusden, in preparation.
31 E. Dickinson, *J. Chem. Soc., Faraday Trans.*, 1995, **91**, 51.
32 E. Dickinson, *Chem. Soc. Rev.*, 1985, **14**, 421.
33 P. G. Wolynes and J. M. Deutch, *J. Chem. Phys.*, 1977, **67**, 733.
34 E. Dickinson, S. A. Allison and J. A. McCammon, *J. Chem. Soc., Faraday Trans. 2*, 1985, **81**, 591.

*Paper* 5/03291A; *Received* 22*nd May*, 1995